Renewable and Sustainable Energy Reviews 84 (2018) 43–53

Contents lists available at ScienceDirect

Renewable and Sustainable Energy Reviews

journal homepage: www.elsevier.com/locate/rser

Fundamentals of bulk heterojunction organic solar cells: An overview of stability/degradation issues and strategies for improvement

Saqib Rafique[a], Shahino Mah Abdullah[a], Khaulah Sulaiman[a], Mitsumasa Iwamoto[b,*]

[a] Low Dimensional Materials Research Centre, Department of Physics, Faculty of Science, University of Malaya, 50603 Kuala Lumpur, Malaysia
[b] Department of Physical Electronics, Tokyo Institute of Technology, 2-12-1 O-Okayama, Meguro-ku, Tokyo 152-8552, Japan

ARTICLE INFO

Keywords:
Bulk heterojunction organic solar cells (BHJ OSCs)
Performance characteristics
Working principle
Stability
Degradation
Strategies to improve

ABSTRACT

In the last few years, the performance of organic solar cells (OSCs) based on bulk heterojunction (BHJ) structure has remarkably improved. However, for a large scale roll to roll (R2R) manufacturing of this technology and precise device fabrication, further improvements are critical. This article highlights the fundamentals of a BHJ OSC, including its working principle and performance characteristics. The importance of stability for the device lifetime is underpinned and different degradation factors affecting the operational life of OSCs are discussed. Lastly, the strategies to improve the stability of OSCs, including the encapsulation of device, morphology control in BHJ layer, interfacial engineering in terms of buffered layers, use of inverted geometry and alternative electrode materials are highlighted. Moreover, a simple mathematical model of degradation trends in OSCs is proposed. This review provides a comprehensive insight into the current status of BHJ OSCs regarding stability/degradation and covers almost all critical aspects that are considered important to understand it.

1. Introduction

Solar energy is believed to have the highest potential among other alternative energy resources such as hydroelectric, biomass and wind energy. It is inexhaustible and environmental friendly, especially, organic solar cells (OSCs) have attracted immense attention as a possible alternative to their inorganic counterparts [1]. Potential for cost effective and fast roll to roll (R2R) production, as well as their light weight and fabrication on flexible substrates, provide them an edge over traditional inorganic solar cells [2–5]. Although power conversion efficiencies (PCEs) of more than 10% have been recently reported [6,7]. However, significant work is required to translate the progress made at lab-scale towards the large scale industrial production [8,9].

An ideal photovoltaic device should possess a consistent performance during its operational lifetime; however, organic semiconductors are often regarded as inherently unstable when they are subjected to the cyclic environmental changes [10]. Undoubtedly, significant degradation pathways have been posited to occur at virtually every layer and interface of OSC devices. Therefore, the stability of the OSCs is of paramount importance to identify and improve the degradation factors affecting the device performance. Until recent years, the search for highly efficient OSC materials and device structures has been of tremendous interest in the OSC community, with device lifetime being largely ignored. Therefore, the scientific community is changing the focus to the stability constraints of the OSCs, largely driven by the recent critical needs to understand and optimize the stability and reliability of organic photovoltaic based products [11–13]. Several strategies have been adopted to improve the performance of OSCs such as synthesis of new donor and acceptor fragments of the photoactive blend [14–16], controlling the morphology of photoactive layer [17–19], employing interfacial layers [20–22], and designing and implementation of new device architectures [23–25]. As a result, despite the limited demonstration of actual large-scale installations of OSC modules, a steady increase in their efficiency and stability is frequently published [26].

This review article discusses fundamental concepts of BHJ OSCs, with a focus on factors limiting the device stability and strategies to improve the stability. Despite the notable progress in both the efficiency and stability, the future of OSCs is uncertain because of several stability challenges. Here we discuss and proposed solutions to these challenges. Firstly, we briefly described the degradation factors that limit the device lifetime, such as morphology of photoactive layer, diffusion of

Abbreviations: BHJ, Bulk heterojunction; FF, Fill factor; HOMO, Highest occupied molecular orbital; HTL, Hole transport layer; J_{sc}, Short circuit current density; L_D, Diffusion length; LUMO, Lowest unoccupied molecular orbital; OSCs, Organic solar cells; P3HT, Poly(3-hexylthiophene-2,5-diyl); PCBM, [6,6]-Phenyl-C61-butyric acid methyl ester; PCDTBT, Poly[N-9′-heptadecanyl-2,7-carbazole-*alt*-5,5-(4′,7′-di-2-thienyl-2′,1′,3′-benzothiadiazole)]; PCE, Power conversion efficiency; PEDOT:PSS, Poly(3,4-ethylenedioxythiophene) polystyrene sulfonate; PV, Photovoltaics; R2R, Roll to roll; V_{oc}, Open circuit voltage; WF, Work function

* Corresponding author.
E-mail address: iwamoto.m.ac@m.titech.ac.jp (M. Iwamoto).

https://doi.org/10.1016/j.rser.2017.12.008
Received 2 November 2017; Accepted 16 December 2017
Available online 29 December 2017

electrodes and interfacial layers, oxygen and water ingress, photo-degradation and mechanical degradation. Lastly, we surveyed and analyzed the strategies to increase the stability, such as encapsulation from outside atmosphere, interfacial engineering to enhance performance, morphology control and use of inverted device architecture.

2. Fundamentals of bulk heterojunction solar cells

A BHJ OSC essentially consists of a multilayer structure in which each layer in the device architecture could be deposited by an individual fabrication technique. The absorber layer is comprised of two constituents; a donor material is usually a conjugated polymer, conjugated pigments or oligomers, and for an acceptor material often fullerene derivatives are used. The photoactive layer is sandwiched between the anode and top low work function (WF) cathode. Often the interfacial layers namely hole transport layer (HTL) and an electron transport layer (ETL) are inserted between the anode-photoactive and cathode-photoactive interfaces, respectively to improve performance and stability of the BHJ OSCs [27]. Over the years, inverted device architecture has also been established for BHJ OSCs. In an inverted device, the bottom transparent electrode serves as the cathode while the top electrode is an anode. The performance of inverted devices is comparable with the normal architecture solar cells; in addition, they also exhibit relatively higher environmental stability. Typical device architecture for normal and inverted solar cells is illustrated in Fig. 1.

2.1. Operation principle

The simplified working principle of BHJ OSC device can be described in at-least four fundamental steps namely (i) photons absorption and exciton formation, (ii) exciton diffusion and splitting, (iii) charge transportation and, (iv) charge collection [27–29]. In a BHJ OSC device, light is usually absorbed by the donor material, *e.g.,* a conjugated polymer. Upon absorption of photons, an electron is excited from the highest occupied molecular orbital (HOMO) to the lowest unoccupied molecular orbital (LUMO). The offset between donor (LUMO) and acceptor (LUMO) must be in the range of 0.1–1.4 eV to generate the electron-hole pairs also known as the excitons. The excitons must diffuse to the donor-acceptor interface where there is sufficient potential energy drop to split these excitons into the free charge carriers, *i.e.,* the electrons and the holes [30]. After splitting into free charge carriers, each carrier must be transported to the respective electrode through the bicontinuous interpenetrating pathway while avoiding recombination and trapping of charges. Some limitations and losses could occur during these steps such as absorption loss due to spectral mismatch, thermalization loss, the insufficient energy required for exciton splitting, and charge recombination, etc. [31]. A detailed description of each of the steps involved from light absorption to the charge carrier collection is presented below.

2.1.1. Light absorption and exciton generation

As the first and essential requirement to achieve high efficiency, the photoactive layer must absorb the maximum of the incoming sunlight. Light is usually absorbed by donor fraction of the BHJ photoactive layer. Due to high absorption coefficient of conjugated polymers (10^7 m^{-1}), they can effectively absorb light at maximum of their absorption spectrum [32] with very low thickness of the photoactive (usually up to 100 nm) layer as compared to their inorganic silicon (an indirect semiconductor) based counterparts where thicknesses of hundreds of micrometres are required. Moreover, the thickness of the polymer based photoactive layer is also limited to 100 nm due to low charge-carrier mobilities in most of the polymers that lead to an absorption of only 60% of the incident light at the absorption maximum (excluding back reflection of the electrode) [32]. In contrast, the inorganic semiconductors can effectively absorb the whole visible solar spectrum [28,32]. Thus, low absorption in conjugated polymers leads to low photocurrent generation. Interestingly, the absorption of light can be enhanced by lowering the band gap of donor polymers that results in absorption of a maximum number of photons that lead to higher PCEs [33,34]. Therefore, materials with lower band gap are necessary to optimize the photon harvesting. For instance, a material with band gap lower than 2 eV is considered as a low band gap material that leads to the possibilities of improving the efficiency of OSCs due to a better overlap with the solar spectrum. For example, a band gap of 1.1 eV can cover 77% of the AM 1.5 solar photon flux as compared to the band gap of 1.9 eV that can hardly cover 30% of the AM1.5 photon flux [34]. Thus, a low band gap material can significantly improve the photocurrent generation.

When the light is illuminated from the transparent electrode side, and upon absorption of the photon; an electron is excited from the HOMO to the LUMO. It is similar to inorganic semiconductors where the electron is excited from valence band to the conduction band. As a result, an electron-hole pair (exciton) with binding energy typically in the range of 0.1–1.4 eV is generated [30]. The excitons are then migrated to the donor-acceptor interface. A schematic representation of the steps in energy production and corresponding band diagram of an OSC is shown in Fig. 2.

2.1.2. Exciton diffusion and charge dissociation

The energy offset in LUMO between donor and acceptor materials breaks the Coulomb attraction that ultimately causes the excitons to dissociate [35–37]. As most of the conjugated polymers exhibit a shorter lifetime of the excitons, the diffusion lengths are limited to a few nanometers (less than 20 nm), which is much shorter than the optical absorption pass length (~ 100–200 nm). It is, therefore, a prerequisite that excitons must be generated within their diffusion length (L_D) for efficient charge generation [2]. Exciton diffusion length is defined as the distance traveled by an exciton before recombination [38]. The reported excitons diffusion length for various conjugated polymers significantly varies from 5 to 20 nm [39–41]. Thus, the thickness of the photoactive layer is very much critical for an efficient charge generation.

In organic semiconductors, photogenerated holes and electrons at the donor/acceptor interface experience a strong Coulomb binding energy [42,43]. These Coulomb bound electron–hole pairs have to be dissociated to get free charge carriers. However, they either recombine

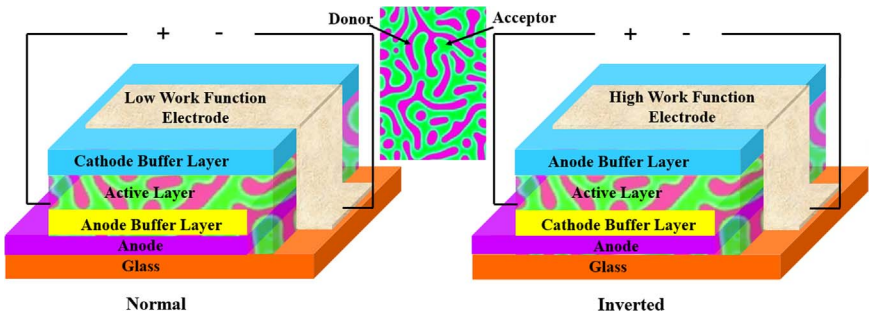

Fig. 1. Device architecture of the (a) normal and (b) inverted BHJ OSCs.

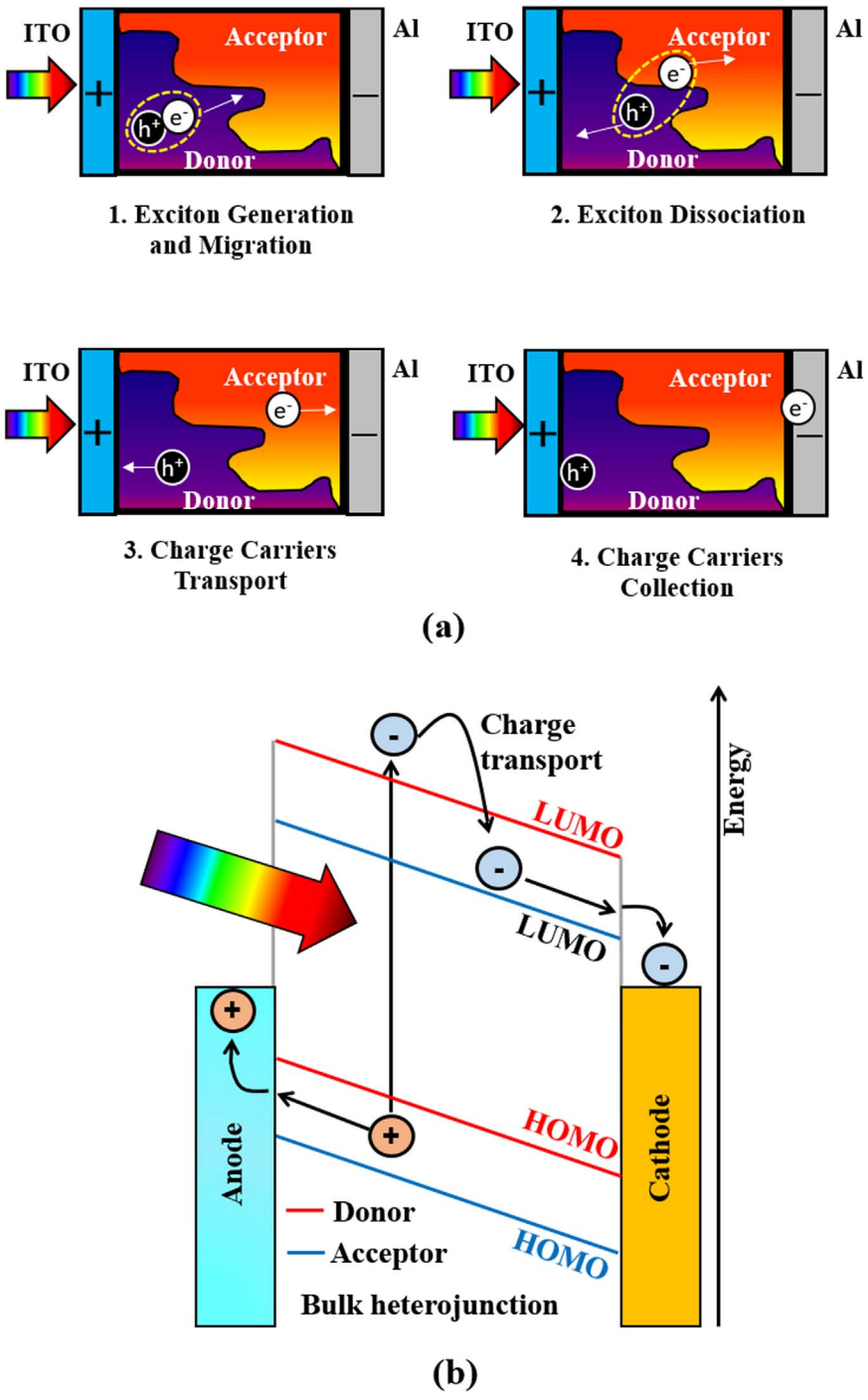

Fig. 2. (a) Steps involved in energy production upon illumination (From exciton generation until charge carriers collection). (b) Band diagram of the photocurrent generation mechanism in a BHJ solar cell.

or dissociate into free charge carriers upon escaping their mutual Coulomb attraction [28,32]. Efficient charge transportation requires efficient dissociation of excitons at the interface. The difference in HOMO and LUMO between donor and acceptor layers creates electrostatic forces at the interface. When materials choice is proper, such differences generate an electric field that leads to the efficient break-up of excitons into electrons and holes [34]. Further, the free electrons are then accepted by the material with higher LUMO level and holes by the material with lower HOMO. Unfortunately, these free charge carriers can lead to recombination or trapping in a disordered interpenetrating organic material while traveling towards the electrodes.

2.1.3. Free charge carriers transport

After the exciton dissociation into free charge carriers, the charges should be transported towards the respective electrodes as shown in Fig. 2. The transportation of charge carriers in organic semiconductors mostly takes place by hopping from one localized state to the next [44,45]. An internal electric field drives transportation of free charge carriers towards their respective electrodes occurred due to the Fermi level difference of the electrodes [46]. In general, a high WF anode and a low WF cathode create an internal electric field that determines the V_{oc} of the cell [38]. Transportation of free charge carriers is either driven by the carrier diffusion or electric field induced drift.

The main bottleneck to the efficient transportation of free charge carriers towards the anode and cathode is their recombination before reaching to their respective electrodes. The charge carriers mobility in the photoactive layer governs both the charge carriers transportation as well as the losses caused due to charge carriers recombination [47]. In

the case of low mobility materials, electrons and holes remain bound by the Coulomb potential. As a result, they cannot overcome their mutual attraction and finally recombine before charge collection at the electrodes [45]. Consequently, the solar cell experiences a significant loss regarding photogenerated current. The path length of photogenerated electrons and holes is in direct proportion to the thickness of the photoactive layer [48]. Charge carrier recombination increases as the photoactive layer gets thicker, resulting in a substantial loss in the device performance [49]. Thus, competition between carrier sweep-out by the internal field and the loss of photogenerated carriers by recombination are the significant issues to overcome for high-efficiency devices [48].

2.1.4. Collection of the charge carriers at the electrodes

Photogenerated charge carriers that do not recombine are finally extracted from the photoactive layer to the respective electrodes. The potential barrier at the photoactive layer/electrodes interface must be reduced to maximize the extraction of charges [28]. Therefore, the WF of the anode should match with the HOMO of the donor material, while the WF of the cathode must match with the LUMO of the acceptor material [38]. If the WFs match well as described, then the contacts are said to be Ohmic contacts. Contrary to this, if there is a mismatch between the anode and cathode with that of donor HOMO or acceptor LUMO, respectively, then no Ohmic contacts would be established. Ultimately, the performance of the solar cells will reduce [32].

The charge collection at the respective electrodes concludes the steps from absorption of light to generation of photocurrent as shown in Fig. 2. The PV performance characteristics such as J_{sc}, $V_{oc,}$ and *FF* are reliant on the photocurrent generation. Therefore, a brief discussion on the performance characteristics of an OSC is presented in Section 2.2.

2.2. Performance characteristics

Three important parameters determine the PCE of a solar cell: The current that reaches to the electrodes without any applied field is termed as the short circuit current (J_{sc}) whereas, open circuit voltage (V_{oc}) is the maximum potential generated by the device. For the current to do work, it must be generated with some potential. The ratio of maximum obtained power to the product of J_{sc} and V_{oc} is known as fill factor (*FF*), and it defines the quality of the device. PCE is defined as the product of these three parameters divided by input power (P_{in}) and denoted by sign (η). Mathematically;

$$\eta = \frac{P_{out}}{P_{in}} = \frac{FF\,(V_{oc} \times J_{sc})}{P_{in}} \quad (1)$$

$$FF = \frac{V_{mpp} \times I_{mpp}}{V_{oc} \times J_{sc}} \quad (2)$$

whereas, V_{mpp} and J_{mpp} (Eq. (2)) are the voltage and current density at the maximum output power, respectively. Fig. 3 shows a typical Current density - Voltage (*JV*) curve for a solar cell. It illustrates the V_{oc}, J_{sc}, *FF*, and the values for J_{Mpp} and V_{Mpp} (J_{Mpp} and V_{Mpp} are the points on the *JV* curve where maximum power is produced). The outlined shaded area in the graph indicates the *FF*. While the product of current and voltage has the highest yield at the maximum power point (M_{PP}) [50]. Below, a brief description for each of them is presented.

2.2.1. Short circuit current density (J_{sc})

The J_{sc} is the maximum photocurrent density generated at zero applied potential (*e.g.,* short circuit conditions when $V_{oc} = 0$) [51] or in other words, it represents the number of charge carriers generated and finally collected at the respective electrodes at zero applied potential [38]. Although, there is no power produced at this point, however, the J_{sc} marks the onset of the power.

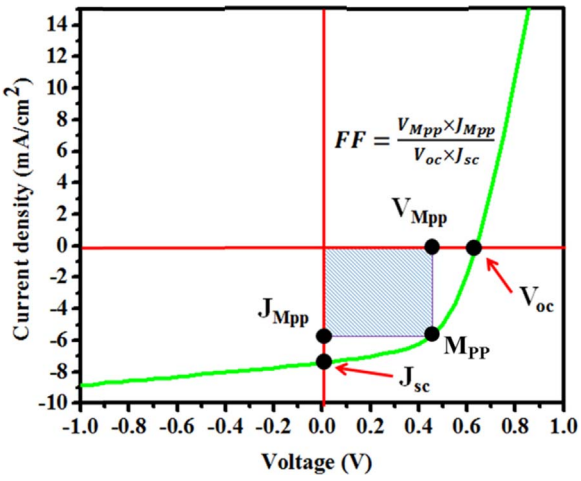

Fig. 3. Typical current density- voltage (*J-V*) curves of an OSC.

2.2.2. Open circuit voltage (V_{oc})

One of the most important factors determining the device efficiency is V_{oc} that is determined when $J = 0$ or it is being open circuited [52]. It is the measure of the maximum of the voltage that a solar cell can extract for an external circuit [53,54]. Although, a generally accepted view is that V_{oc} in the BHJ OSCs originates from the energy offset between the HOMO of the donor and LUMO of the acceptor material [55], however, early studies reveal that the V_{oc} is determined by the difference in the WFs of the two electrodes [56], the so called metal-insulator-metal (MIM) model [57,58].

2.2.3. Fill factor (FF)

The *FF* is an important parameter that determines the PCE of an OSC. PCE of an OSC is calculated from its *J-V* characteristics as a product of J_{sc}, $V_{oc,}$ and *FF*. Moreover, the shape of the *J-V* characteristics of an OSC is characterized by the *FF* that is the ratio of the maximum output power to the product of J_{sc} and V_{oc} [59]. The shape of the *J-V* curve determines how "difficult" or how "easy" the photogenerated carriers can be extracted out of a solar cell device and ideally *FF* should be 100% when the *J-V* curve is exactly a rectangle [60].

2.2.4. Power conversion efficiency (PCE)

Finally, the most discussed performance parameter of a solar cell device is its PCE. It is defined as the percentage of input irradiation (P_{in}) that is converted into the output power and expressed as the product of V_{oc}, J_{sc}, and *FF* divided by the input power (P_{in}).

In summary, these key performance parameters of OSCs play a major role in determining and optimizing the performance of solar cells. Every single factor contributing towards the efficiency of the device has to be enhanced by improving electrodes, BHJ material, every layer, and interfaces to achieve the optimum performance.

3. Stability/degradation of BHJ OSCs

OSCs have exponentially evolved in terms of efficiency and stability. Whereas the PCE has been increased by almost a factor of ten exceeding 10%, a lifetime of the OSCs has also approached several thousand hours under favorable circumstances [13,61]. However, stability is still a bottleneck to the widespread commercialization of OSCs. While promising achievements in the PCEs of OSCs, above 10% value only represents the initial performance of the OSCs – how the PCE of the solar cell degrades with time is also of critical importance. The energy output of a solar cell device is the product of its efficiency and lifetime stability, illustrated in Fig. 4. Therefore device stability is of paramount importance in OSCs and inferior device stability remains a great challenge to compete the inorganic silicon based solar cells in the

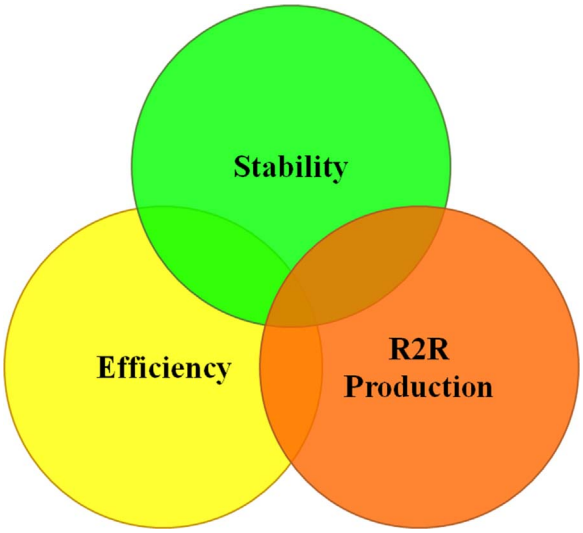

Fig. 4. Key areas of research pertaining to OSCs.

photovoltaic industry. Moreover, the fabrication techniques must be compatible with the R2R production for the widespread commercialization of OSCs.

Studying the stability of OSCs helps in understanding how a device degrades during operation. Device instability occurs due to a range of complex phenomena that are in play simultaneously of which presumably many have not been yet identified [62]. OSCs are highly sensitive to even a small degree of degradations that makes degradation factors extremely critical for device operation and thus should be completely removed or at least reduced to improve device lifetime [63].

Obtaining longer operational lifetime in OSCs is challenging, as degradation mechanism in OSCs is rather complex and cannot be explained by a single process. It may include factors affecting active layer, the transport layers, the contacts and the interface of every layer with the adjacent layers [64,65]. In general, degradation factors in OSCs can be distinguished to be either intrinsic or extrinsic. Examples of these factors are oxygen and water diffusion [66], electro-migration induced shunts, oxidation and rusting of Al electrode due to moisture [67], indium diffusion from anode due to acidic PEDOT:PSS [68], swelling of water-soluble layers as well as corrosion and delamination of the metal contacts due to oxygen and water ingress [69]. Moreover, thermal and photoinduced degradation of active layer under illumination in ambient conditions, active layer intrinsic chemical evolution, photo-bleaching and mechanically induced stress also occur in OSCs [70–72]. Both types of degradation are mass-flow (diffusion) processes. This section briefly covers some of the most pronounced degradation effects, while the schematic representation of some of the degradation factors limiting the device stability is shown in Fig. 5.

3.1. Intrinsic degradation

OSCs are currently the ultimate in terms of complexity, and they exhibit the most uncontrollable situation in terms of stability. So far, most of the research is focused on effects of extrinsic degradation factors such as temperature, light, oxygen, and humidity on the photoactive layer, electrodes, and interfaces. However, less attention has been given to the intrinsic degradation mechanisms. In general, the intrinsic degradation arises from thermal diffusion of constituent materials at interfaces of OSCs [12]. It occurs due to changes in the properties of the interface between layers of the stacking owing to internal modification of the materials used [73]. Even after encapsulation (to avoid oxygen and moisture ingress), intrinsic degradation in photoactive layer can occur due to light or by the elevated temperatures due to continuous exposure to sunlight [74]. It includes inter-diffusion of electrodes [75], interfacial layers [68], phase-separation at organic-cathode interface and change in the nanoscale morphology of BHJ constituents [12,76]. Moreover the thermally activated phase separation and the photochemical damages occur in the BHJ films [77], which can cause further deterioration of mechanical properties such as brittleness and stiffness in the photoactive layer [78,79].

Photoactive layer is the most critical component of OSCs, and is comprised of donor, acceptor and donor/acceptor mixed phase. It possesses metastable phase separation due to strong mobility of its organic constituents. Therefore, often high boiling point additive solvents are added in the photoactive blend to increase the efficiency. However, these additives significantly hamper the device stability [80–82]. Some of these additives are highly sensitive to light and can directly saturate the polymer conjugated backbone or be trapped by the fullerene moieties. In addition, they can accelerate the photo-oxidation of the BHJ layer [81,83].

Similar to photoactive layer, electrodes and interfacial layers also possess mobility resulting in severe device instability [84]. Widely used PEDOT:PSS is highly acidic and hygroscopic that upon contact with ITO anode, corrodes its surface. This leads to diffusion of indium (*e.g.,* dissolution of In_2O_3) into the photoactive layer that results in trapping of charge carriers [85–87]. Al is normally employed as a cathode that readily gets oxidized to form Al_2O_3. Water can diffuse through pinholes and voids to the underneath layers that ultimately lowers the device lifetime [62]. Moreover, water ingress from the edges through the PEDOT:PSS also oxidizes the cathode and significantly reduces the J_{sc} [67,88,89]. Such diffusion of electrodes and interfacial layers can drastically reduce the device lifetime by changing the energy levels of interfacial layers as well as causing charge carrier trapping and recombination [90].

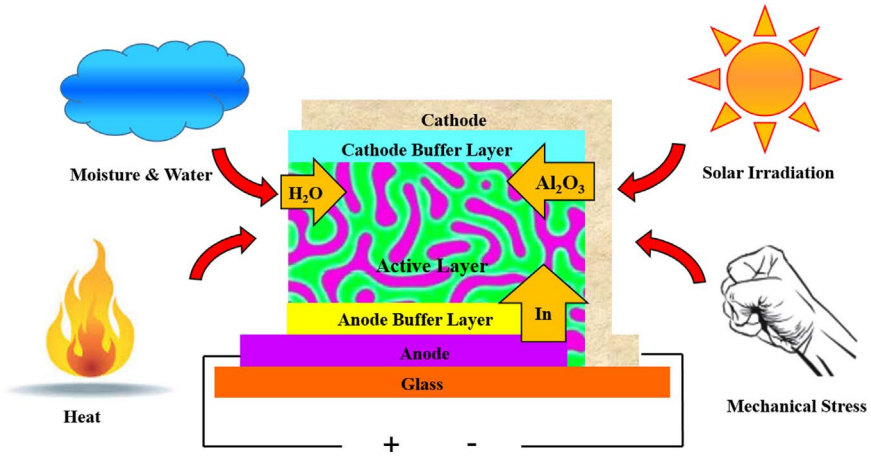

Fig. 5. Degradation factors that affect the device stability.

3.2. Extrinsic degradation

An ideal OSC device should possess consistent performance over time when it is exposed to cyclic changes in the environment such as light/dark, hot/cold, and dry/humid conditions. However, the fact is opposite and with the emergence of new photovoltaic technologies such as OSCs, the stability of these devices is compromised as compared to silicon based solar cells [13,91]. The poor long-term stability of OSCs needs to be overcome for their successful commercialization. Most importantly, an unanticipated delay in the device performance during its initial operation, the so called 'burn-in' loss, is one of the causes for the device shorter lifetime [92]. A second phase starts after the burn-in phase that shows a linear trend in degradation. The slope of this linear trend determines the lifetime of an OSC, which is chosen to be the time over which device efficiency reduces to the 80% (T_{80}) of the post burn-in efficiency [93]. Extrinsic stability can only be ensured with proper encapsulation of the device from the outside environment because unencapsulated device rapidly degrades in ambient air and the device efficiency plunges down to negligible within few minutes [94]. Some of the degradation factors affecting device performance are briefly discussed below.

3.2.1. Oxygen and water

Oxygen and water, extrinsic to OSCs are some of the known degradation factors affecting device stability [13,95]. Typically, the constituents of an OSC are subjected to degradation upon exposure to ambient atmosphere. Molecular oxygen and water cause chemical degradation (photo-oxidation) of the organic layers and interfaces, which consequently will disrupt the delicate electrochemical processes that are vital for the photovoltaic performance [13]. Moreover, the photo-oxidation of the active layer also alters its absorption, energy levels and charge carrier mobilities such as quenching the polymer excited state and a severe impact on electronic properties of fullerene domains [10] as well as aggregation of fullerene domains [96]. Consequently, the device performance can be severely hampered. In addition, hole concentration can be increased due to oxidation of active layer that leads to a decrease in the density of deeper traps for electrons and eventually reduces the *FF* and V_{oc} of a device [97,98].

Oxygen and water diffuse through the whole device and equally damage the functionality of each layer [99]. The low *WF* metal cathode gets oxidized due to oxygen ingress. Consequently, an insulating metal oxide layer is formed that creates a transport barrier, ultimately an S-shaped *I-V* curve is induced and the performance of the device gets degraded [100]. Also, the formation of pinholes and voids in the metal layer facilitates the diffusion of water and oxygen to the underneath layers [88]. Moreover, PEDOT:PSS is known to be hygroscopic, and the absorbed water can further penetrate into the whole device. The PEDOT:PSS could be phase separated, with the PEDOT rich phase being responsible for most of the interfacial degradation in the presence of water and oxygen [63]. In addition, the photo-oxidation of the active layer, the formation of the metal oxide insulating layer and phase separation leads to a reduction in the donor-acceptor interfaces, which could potentially harm the exciton dissociation. Thus the performance of an OSC is significantly reduced [96].

3.2.2. Photo-degradation upon irradiation

Light-induced degradations are one of the most crucial issues to be addressed because any photovoltaic device is inevitably operated under the light exposure. OSCs are proven to be unstable upon irradiation, and severe deterioration of device efficiency during 100 h of light exposure has been reported by recent studies conducted by Yamanari et al. [101] This is referred as the burn-in photo-degradation and proves to be one of the major barriers to the successful commercialization of OSCs [102]. Unfortunately, light irradiation accelerates the degradation of OSCs in a number of ways. Firstly, as discussed earlier, continuous illumination elevates the temperature and causes thermally induced degradation that eventually boosts the intrinsic degradation of OSCs [76]. Secondly, the irradiation also degrades the organic constituents of an OSC and causes the oxidation of photoactive material near Al interface [103]. Moreover, excessive illumination also accelerates the diffusion of oxygen and moisture in the bulk of photoactive layer [89,104].

Recently, Córcoles et al. [105] studied the influence of varied wavelength of solar cell spectrum on the stability of P3HT: PCBM based OSCs. Their study reveals that certain wavelengths of solar spectrum are more harmful to the device stability. For example, blue and ultraviolet wavelengths accelerate the device degradation. Madsen et al. [106] demonstrated in their recent work that light intensity also influences the stability of an OSC and the degradation rate linearly scales with the light intensity. Above all, the key reason for light induced instability is the photochemical and photophysical degradation that occur in every layer and interfaces [90]. Further, in this context, several reports confirm that photo-oxidation reaction in the photoactive layer is the main reason that hampers the device degradation [107,108]. The device faces several consequences of these photo-oxidation reactions such as low photo-absorption due to the altered donor and acceptor structures that eventually decreases the excitons generations [109]. Moreover, these reactions alter the energy levels of donor and acceptor materials as the two components do not get equally affected by these photo-oxidation reactions. Consequently, energy level alignment between the donor and acceptor fractions gets disrupted [110]. Finally, photo induced oligomerization of fullerene component and photolysis of donor fraction in the active layer occur that cause the instability of OSCs upon irradiation [111,112].

In addition to chemically induced photo-degradation, Adachi et al. and Kumar et al. [113,114] revealed physically induced photo-degradation of the devices that occur due to carrier accumulation, resulting in severe degradation in solar cell performance. Their studies established this fact that amount of accumulated charge carriers and degree of degradation of an OSC are closely related to each other.

3.2.3. Mechanical degradation

Mechanical degradation is the less studied mode of degradation as compared to other extrinsic and intrinsic degradation modes. However, it is essential to address for the *R2R* manufacturing and the operational stability of OSCs, in particular for the portable and outdoor applications [77]. The flexible modules of OSCs often go through the substantial bending, shearing and deformation, and therefore, require resistance to these mechanically induced degradations. Mechanically induced degradations (stress) could affect polymer-fullerene layer, the interfacial layers, electrodes and the interfaces [90]. Moreover, in case of their installation and exposure to the real world atmospheric conditions, the devices could face severe mechanical degradation including delamination, cracking, scratches, punctures and bends [115]. The punctures and edge delamination facilitate the water and oxygen ingress that eventually cause further delamination of the modules [26]. Consequently, as discussed earlier, the penetration of oxygen and water equally affect all the layers and their interfaces.

As long as the photoactive layer is concerned, Awartani et al. [116] in their recent work highlighted two critical mechanical parameters of BHJ photoactive layer namely stiffness and ductility that are correlated to the device performance. Adequate knowledge of these factors is essential to provide insight into the performance, stability, and underlying degradation phenomena that could occur during the material's service life [117]. Their study concluded that the P3HT:PCBM based blend increased the elastic modulus and lowered the crack onset strain. Bruner et al. [118] recently reported their findings on molecular intercalation and cohesion of BHJ OSCs. Their findings suggest that polymer-fullerene BHJ layer is cohesively weak resulting in thermo-mechanical failure within the BHJ layer and is influenced by the formation of a bimolecular crystal phase within the BHJ layer.

Dupont et al. [119] discussed the importance of inter-layer adhesion

in *R2R* processed OSCs. Their work suggests that poor adhesion between adjacent layers may result in loss of device performance due to delamination driven by the thermomechanical stresses in the device. In particular, their study revealed that interface of BHJ layer with the PEDOT: PSS was found to be the weakest. In summary, all the above degradation factors comprise an intriguing aspect of interdisciplinary research that requires a team of experts in organic chemistry, device physics, polymer science, interfacial engineering and microstructural determination.

4. Strategies to improve device stability

It is vital that for the successful performance of an OSC, the device must be extrinsically and intrinsically stable. The OSC modules must resist to mechanical, oxidative, irradiation, thermal and photochemical instabilities. The electrodes, the interfacial layers and most importantly the photoactive layer and their interfaces should not be susceptible to degradation factors. Several strategies have been adopted to address the stability concerns associated with the operational lifetime of an OSC. This section briefly describes a few strategies to improve the intrinsic and extrinsic stability of an OSC.

4.1. Encapsulation

Encapsulation is one of the key measures that are taken to ensure extrinsic stability. Oxygen and water are the known degradation factors; therefore, it is the standard procedure of fabrication to encapsulate the devices in various ways [13]. In addition, it prevents the device from mechanical instabilities such as scratches and bending. However, the photovoltaic properties of an encapsulated device depend on the encapsulation material and method [90]. In general, OSCs are encapsulated with the glass plates; however, it is not compatible with flexible solar cell modules. Therefore, in recent years, organic based encapsulation materials have been employed to protect OSCs [120–122]. Elkington et al. [123] employed a bisphenol A-based epoxy resin as an encapsulation material on BHJ OSCs. The encapsulant proved to be a barrier against the degradation in air. Similarly, Peters et al. [124] demonstrated a highly stable PCDTBT:$PC_{71}BM$ based device by using UV curable epoxy glue as a top encapsulation layer. The device lifetime approached to around 7 years that is one of the longest ever reported life of an OSC. Recently, metal oxides along with MgF_2 in a layered structure [125] and GO [126] have been employed to encapsulate the OSCs that lead to the highly stable device exhibiting several hundred hours of operational life. Combination of organic-inorganic materials such as epoxy resin and glass can also be used as an encapsulant [94,127].

4.2. Interfacial engineering to enhance performance of OSCs

The basic structure of an OSC comprises of photoactive layer sandwiched between anode and cathode. However, it is now considered as essential to insert interfacial layers at the interface of electrodes and the photoactive layer, making them an integral part of BHJ OSCs. However, most commonly used interfacial materials are susceptible to the degradation and significantly reduce the device performance. Therefore, several alternatives have been explored during the past few years to address stability concerns associated with pristine interfacial materials.

4.2.1. Optimization of HTL

PEDOT:PSS is the most commonly employed HTL material, but it favors the device degradation due to its acidic and hygroscopic nature. Ultimately, it corrodes the underneath ITO that further diffuses into the photoactive layer. Therefore, several alternative materials have been reported to work as HTLs in OSCs. Among them, metal oxides based HTLs are the most studied alternatives to the acidic PEDOT:PSS [128,129]. Metal oxides such as NiO [130], V_2O_5 [131], WO_3 [132] and MoO_3 [133] have been widely used as HTLs in OSCs [134]. All these materials can be processed from solution, and thus are compatible with *R2R* production [135–137]. Recently, GO has been employed as a potential HTL material in BHJ OSCs [138,139]. GO is an oxidized state of graphene that possesses excellent properties such as high transparency and excellent mechanical properties to act as an HTL [140]. Another alternative is to use a combination of metal oxide/GO along with PEDOT:PSS to complement the drawbacks of each of the individual materials [141,142].

4.2.2. Optimization of ETL

LiF or Ca and ZnO are the most commonly employed ETLs in conventional and inverted geometry BHJ OSCs, respectively. These materials are unstable in the ambient atmosphere due to their reactivity with oxygen, water (for LiF and Ca), air and light (for ZnO) [90]. In addition, vacuum deposition is not compatible with *R2R* manufacturing. In this context, metal oxides such as CrO_x [143], Cs_2CO_3 [144], TiO_2 [145] and electron extracting polymers have been employed as alternative ETLs [146]. Moreover, ZnO can be modified in a number of ways to overcome the stability issues associated with the single ZnO ETL [12]. Metal doping of ZnO is commonly used to enhance the electron transport characteristics [147]. In addition, several other structures of ZnO such as nanowires, nanorods, nanoflakes, and nanowalls are also reported in the literature as ETLs [148]. Like HTL, GO can also be used as an ETL material to improve the efficiency and stability of OSCs. Wang et al. [149] demonstrated PCDTBT:$PC_{71}BM$ BHJ OSCs employing an ETL of stretchable GO by stamping transfer. The resultant device showed enhanced efficiency and stability as compared to a pristine device without any interlayer. Efficacy of GO as an ETL has been reported by several other works [134,150].

4.3. Morphology control in the BHJ photoactive layer

Photoactive layer comprises of BHJ of polymer-fullerene is the most important component of an OSC. Although, BHJ OSCs are showing promising results regarding efficiency and stability, however, the morphology of each donor-acceptor material differs significantly, particularly in relation to domain size and degree of interpenetration between domains [151]. Due to shorter diffusion length of excitons, the photoactive layer must comprise of interpenetrating network morphology consisting of optimized domain size of both donor and acceptor constituents to facilitate the migration of excitons to the donor- acceptor interface and their splitting into the free charge carriers so that the charge carriers can be extracted. Ideally, the domain size of donor-acceptor fragments must be in the range of 10–20 nm [152].

The inclusion of the third component in addition to donor-acceptor fragments is a popular approach to enhance the device performance [153–155]. A third component could be a cross-linked to enhance the thermal stability [156,157], modified fullerene derivatives acting as cross linker to thermally stabilize the device [158,159], inclusion of compatibilizers to enhance the thermal and mechanical stabilities [160,161] and employing insulator polymer as a third agent to simultaneously increase thermal and mechanical stabilities [162]. In addition, to improve the thermal and mechanical stability, the inclusion of the third agent can also enhance the air and photostability [163,164]. Moreover, solvent additives also enhance the device performance. In this context, Peet et al. [165] incorporated a few volume percent of alkanethiols in the PCPDTBT:PCBM blend that results in an enhanced efficiency from 2.8 to 5.5% through altering the bulk heterojunction morphology. Moreover, optimization of processing parameters of the photoactive blend such as preparation of the solution, formation of thin film, and post treatment such as thermal annealing can enhance the stability of an OSC [90,166].

4.4. Use of inverted geometry and alternative electrodes to enhance stability

The normal architecture BHJ OSC consists of a low *WF* Al electrode that is sensitive to oxygen and moisture. As a result, it reacts with atmospheric oxygen and water, and they further diffuse into the whole device through the top cathode. Therefore, inverted geometry has been developed to overcome this issue in which the position of cathode and anode is interchanged. The inverted device showed much better air stability as compared to the normal architecture OSCs while the efficiencies are still comparable with that of normal architecture [167–170].

As discussed earlier, Al is susceptible to oxygen and water. Therefore, silver has been widely used as an alternative anode material. As a noble metal, silver is more stable than Al upon exposure to the ambient atmosphere [171]. Recently, Yeom et al. [172] employed silver and a gold top electrode in PTB7:$PC_{71}BM$ based inverted OSCs and the resultant devices exhibited high stability and photovoltaic performance. Sio et al. [173] in their recent work employed MoO_3/Ag anode in P3HT:PCBM based inverted device that led to enhanced stability.

An in-depth knowledge of degradation mechanism in OSCs is critical in achieving high stability and efficiency in BHJ OSCs. Furthermore, aforementioned strategies must be adopted to mitigate the degradation factors and ensure the higher operational stability of the solar cells.

5. Proposed mathematical degradation model

As mentioned in earlier sections, there are many issues to overcome to achieve high stability and efficiency in BHJ OSCs. The performance of the OSCs gradually degrades with time. One of the best approaches is to model the degradation behavior of OSCs to predict their degradation trends. Therefore, we here briefly introduce our study concerning modeling of OSC degradation by the empirical behavior of the OSCs characteristics. In general, the degradation behavior of an OSC can be modelled by using fundamental mathematical equations that describe the degradation due to intrinsic material properties in order to evaluate its lifetime. Normally, the degradation of OSC devices exhibit the monotonously decaying behavior, and the following expression can mathematically represent it:

$$\frac{\eta}{\eta_o} = \frac{1}{e^{\lambda t}} \tag{3}$$

where η/η_o, t, and λ are the normalized degradation, the time of degradation in hours, and a decay rate, respectively. It is important to note that the λ is a decay rate that has an inverse relation with the exponential time constant or means a lifetime ($\lambda = 1/\tau$). This means, at $t = 0$, $\eta/\eta_o = 1$, whereas in the limit $t \to \infty$, the $\eta/\eta_o = 0$.

By having a decay factor (e^{λ}), it will describe the exponential decay trend for degraded OSCs that corresponds to a decay rate, λ. Thus, the degradation behavior for a given final normalized degradation with $\eta/\eta_o = 1\text{-}E$ against time of degradation can be written as;

$$\frac{\eta}{\eta_o} = \frac{E}{e^{\lambda t}} + (1-E) \tag{4}$$

where E is the percentage of average PCE loss. In Eq. (4), the first expression on the right-hand side represents the trend of degradation rate until the normalized degradation (η/η_o) remains to be constant, while the second expression on the right-hand side represents the limit of degradation in a period of time (Fig. 6).

From this expression, the limit of degradation at a particular time can also be known as degradation-limited time or t_s that mean when $t \leq t_s$, then $\eta/\eta_o \sim 1/e^{\lambda t}$, but when $t > t_s$, then $\eta/\eta_o = 1 - E$. For determining t_s, it can be extracted from the graft in which it is located at the starting point of the degradation limit where the PCE starts to be constant and fixed onwards after it has undergone a reverse exponential trend of degradation (or a decay function). At the same time, the value

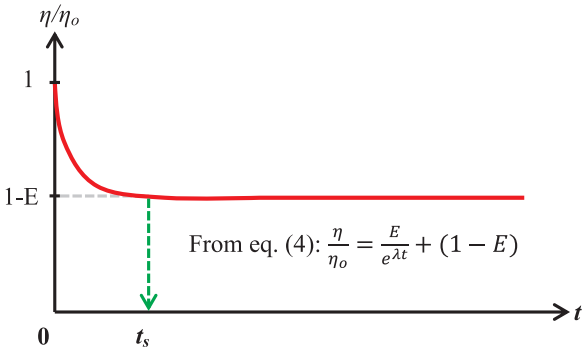

Fig. 6. The plot of degradation trend as expressed by Eq. (4).

of t_s could determine the value of λ (decay or degradation rate) by plotting the following equation:

$$\ln\left(\frac{1}{\eta/\eta_o}\right) = \lambda t \tag{5}$$

From the plot of ln $1/(\eta/\eta_o)$ vs. t, the slope value at t_s will be equal to the value of λ. Above mathematical model of degradation would provide a general view of how OSCs stability last after a period of time. In practical application, it might behave differently than what we proposed here, and further derivation on various degradation trends can be made based on this model.

In summary, to achieve high efficiency and stability of OSCs for large scale production, all of the aforementioned degradation factors must be addressed regarding the issues we discussed in earlier sections. Moreover, further in-depth investigation of device degradation mechanisms is required. As of today, OSCs have already possessed PCEs of more than 10%, and enhancing the lifetime of OSCs will provide an excellent opportunity to realize future industrial manufacture.

6. Conclusions

OSCs have made tremendous progress in almost every aspect. Among OSCs, devices employing BHJ structure have attracted extensive scientific and commercial attractions in recent years. It has become a potential approach to remarkably increase the device performance in terms of efficiency, stability and production cost. Under optimized conditions device efficiency of above 10% and several thousand hours of a lifetime has already been reported. In this review, fundamental aspects of BHJ OSCs ranging from device physics, performance characteristics, stability/degradation mechanisms and strategies to improve device performance, have been discussed. We also proposed a simple mathematical approach that describes the degradation trends in OSCs.

The improvement in the device performance can be attributed to the development of new organic semiconductor materials specifically synthesized to use in OSCs. Moreover, it is also attributed to the development of optimized device physics framework that enables the rational approach to the design of OSC structure including photoactive and transport layers, electrodes, interfaces and choice of suitable material for every layer and interface. The multistep process from light absorption to the charge extraction has been examined largely, and factors affecting this whole process are briefly discussed. Further, the origin of performance characteristics of a BHJ OSC such as V_{oc}, J_{sc}, *FF,* and η has been highlighted.

The intrinsic and extrinsic degradation effects that arise either from material's properties such as migration of constituent materials at interfaces of OSCs or extrinsic factors such as molecular oxygen and water ingress, heat, light irradiation and mechanical stress have been summarized. Most of these factors are thermodynamic, oxidative, photochemical, morphological and mechanical modes of degradation. Furthermore, this review highlights the strategies to improve the device

performance in terms of improving the stability while mitigating the device degradation factors.

Acknowledgement

This work is supported by High Impact Research (HIR) Grant UM.S/625/3/HIR/MoE/SC/26 with account number UM.0000080/HIR.C3 from the Ministry of Education, Malaysia. The financial support from Postgraduate Research Grant PPP University of Malaya with Grant number PG107-2015B is also acknowledged.

References

[1] Bulavko G, Ishchenko AA. Organic bulk heterojunction photovoltaic structures: design, morphology and properties. Russ Chem Rev 2014;83:575.
[2] Scharber MC, Sariciftci NS. Efficiency of bulk-heterojunction organic solar cells. Prog Polym Sci 2013;38:1929–40.
[3] Shivanna R, Shoaee S, Dimitrov S, Kandappa SK, Rajaram S, Durrant JR, et al. Charge generation and transport in efficient organic bulk heterojunction solar cells with a perylene acceptor. Energy Environ Sci 2014;7:435–41.
[4] Lin Y, Li Y, Zhan X. Small molecule semiconductors for high-efficiency organic photovoltaics. Chem Soc Rev 2012;41:4245–72.
[5] Peet J, Heeger AJ, Bazan GC. "Plastic" solar cells: self-assembly of bulk heterojunction nanomaterials by spontaneous phase separation. Acc Chem Res 2009;42:1700–8.
[6] Liu C, Yi C, Wang K, Yang Y, Bhatta RS, Tsige M, et al. Single-junction polymer solar cells with over 10% efficiency by a novel two-dimensional donor–acceptor conjugated copolymer. ACS Appl Mater Interfaces 2015;7:4928–35.
[7] Rohr S. Heliatek consolidates its technology leadership by establishing a new world record for organic solar technology with a cell efficiency of 12%. Dresden, Germany: Press Release Heliatek GmbH; 2013.
[8] Cook TR, Dogutan DK, Reece SY, Surendranath Y, Teets TS, Nocera DG. Solar energy supply and storage for the legacy and nonlegacy worlds. Chem Rev 2010;110:6474–502.
[9] Galagan Y, Coenen EW, Zimmermann B, Slooff LH, Verhees WJ, Veenstra SC, et al. Scaling up ITO-free solar cells. Adv Energy Mater 2014;4.
[10] Reese MO, Nardes AM, Rupert BL, Larsen RE, Olson DC, Lloyd MT, et al. Photoinduced degradation of polymer and polymer–fullerene active layers: experiment and theory. Adv Funct Mater 2010;20:3476–83.
[11] Katz E, Gevorgyan S, Orynbayev M, Krebs FC. Out-door testing and long-term stability of plastic solar cells. Eur Phys J Appl Phys 2006;36:307–11.
[12] Cao H, He W, Mao Y, Lin X, Ishikawa K, Dickerson JH, et al. Recent progress in degradation and stabilization of organic solar cells. J Power Sources 2014;264:168–83.
[13] Jørgensen M, Norrman K, Gevorgyan SA, Tromholt T, Andreasen B, Krebs FC. Stability of polymer solar cells. Adv Mater 2012;24:580–612.
[14] Liang Y, Xu Z, Xia J, Tsai ST, Wu Y, Li G, et al. For the bright future—bulk heterojunction polymer solar cells with power conversion efficiency of 7.4%. Adv Mater 2010;22.
[15] Shang H, Fan H, Liu Y, Hu W, Li Y, Zhan X. A solution-processable star-shaped molecule for high-performance organic solar cells. Adv Mater 2011;23:1554–7.
[16] He Y, Chen H-Y, Hou J, Li Y. Indene- C60 bisadduct: a new acceptor for high-performance polymer solar cells. J Am Chem Soc 2010;132:1377–82.
[17] Ma W, Tumbleston JR, Ye L, Wang C, Hou J, Ade H. Quantification of nano-and mesoscale phase separation and relation to donor and acceptor quantum efficiency, Jsc, and FF in polymer: fullerene solar cells. Adv Mater 2014;26:4234–41.
[18] Sun Y, Welch GC, Leong WL, Takacs CJ, Bazan GC, Heeger AJ. Solution-processed small-molecule solar cells with 6.7% efficiency. Nat Mater 2012;11:44–8.
[19] Cheng P, Hou J, Li Y, Zhan X. layer-by-layer solution-processed low-bandgap polymer-PC61BM solar cells with high efficiency. Adv Energy Mater 2014;4.
[20] Yin Z, Wei J, Zheng Q. Interfacial materials for organic solar cells: recent advances and perspectives. Adv Sci 2016.
[21] Page ZA, Liu Y, Duzhko VV, Russell TP, Emrick T. Fulleropyrrolidine interlayers: tailoring electrodes to raise organic solar cell efficiency. Science 2014;346:441–4.
[22] Lian J, Yuan Y, Peng E, Huang J. Interfacial layers in organic solar cells. In: Organic and hybrid solar cells. Springer; 2014. p. 121–76.
[23] You J, Dou L, Yoshimura K, Kato T, Ohya K, Moriarty T, et al. A polymer tandem solar cell with 10.6% power conversion efficiency. Nat Commun 2013;4:1446.
[24] He Z, Xiao B, Liu F, Wu H, Yang Y, Xiao S, et al. Single-junction polymer solar cells with high efficiency and photovoltage. Nat Photonics 2015;9:174–9.
[25] Yang T, Wang M, Duan C, Hu X, Huang L, Peng J, et al. Inverted polymer solar cells with 8.4% efficiency by conjugated polyelectrolyte. Energy Environ Sci 2012;5:8208–14.
[26] Hösel M, Søndergaard RR, Jørgensen M, Krebs FC. Failure modes and fast repair procedures in high voltage organic solar cell installations. Adv Energy Mater 2014;4.
[27] Facchetti A. Polymer donor–polymer acceptor (all-polymer) solar cells. Mater Today 2013;16:123–32.
[28] Deibel C, Dyakonov V. Polymer? Fullerene bulk heterojunction solar cells. Rep Progress Phys 2010;73:096401.
[29] Dou L, You J, Hong Z, Xu Z, Li G, Street RA, et al. 25th anniversary article: a decade of organic/polymeric photovoltaic research. Adv Mater 2013;25:6642–71.
[30] Mayer AC, Scully SR, Hardin BE, Rowell MW, McGehee MD. Polymer-based solar cells. Mater Today 2007;10:28–33.
[31] Siddiki MK, Li J, Galipeau D, Qiao Q. A review of polymer multijunction solar cells. Energy Environ Sci 2010;3:867–83.
[32] Blom PW, Mihailetchi VD, Koster LJA, Markov DE. Device physics of polymer: fullerene bulk heterojunction solar cells. Adv Mater 2007;19:1551–66.
[33] Brabec CJ, Winder C, Sariciftci NS, Hummelen JC, Dhanabalan A, van Hal PA, et al. A low-bandgap semiconducting polymer for photovoltaic devices and infrared emitting diodes. Adv Funct Mater 2002;12:709–12.
[34] Yeh N, Yeh P. Organic solar cells: their developments and potentials. Renew Sustain Energy Rev 2013;21:421–31.
[35] Ohkita H, Ito S. Exciton and charge dynamics in polymer solar cells studied by transient absorption spectroscopy. In: Organic solar cells. Springer; 2013. p. 103–37.
[36] Gao F, Inganäs O. Charge generation in polymer–fullerene bulk-heterojunction solar cells. Phys Chem Chem Phys 2014;16:20291–304.
[37] Dimitrov SD, Durrant JR. Materials design considerations for charge generation in organic solar cells. Chem Mater 2013;26:616–30.
[38] Fung DD, Choy WC. Introduction to organic solar cells. In: Organic solar cells. Springer; 2013. p. 1–16.
[39] Halls J, Pichler K, Friend R, Moratti S, Holmes A. Exciton diffusion and dissociation in a poly (p-phenylenevinylene)/C60 heterojunction photovoltaic cell. Appl Phys Lett 1996;68:3120–2.
[40] Haugeneder A, Neges M, Kallinger C, Spirkl W, Lemmer U, Feldmann J, et al. Exciton diffusion and dissociation in conjugated polymer/fullerene blends and heterostructures. Phys Rev B 1999;59:15346.
[41] Stübinger T, Brütting W. Exciton diffusion and optical interference in organic donor–acceptor photovoltaic cells. J Appl Phys 2001;90:3632–41.
[42] Clarke TM, Durrant JR. Charge photogeneration in organic solar cells. Chem Rev 2010;110:6736–67.
[43] Deibel C, Strobel T, Dyakonov V. Role of the charge transfer state in organic donor–acceptor solar cells. Adv Mater 2010;22:4097–111.
[44] Baranovskii S, Cordes H, Hensel F, Leising G. Charge-carrier transport in disordered organic solids. Phys Rev B 2000;62:7934.
[45] Pivrikas A, Sariciftci NS, Juška G, Österbacka R. A review of charge transport and recombination in polymer/fullerene organic solar cells. Progress Photovolt: Res Appl 2007;15:677–96.
[46] Zhou Y, Eck M, Krüger M. Bulk-heterojunction hybrid solar cells based on colloidal nanocrystals and conjugated polymers. Energy Environ Sci 2010;3:1851–64.
[47] Mandoc M, Koster L, Blom P. Optimum charge carrier mobility in organic solar cells. Appl Phys Lett 2007;90:133504.
[48] Cowan SR, Banerji N, Leong WL, Heeger AJ. Charge formation, recombination, and sweep-out dynamics in organic solar cells. Adv Funct Mater 2012;22:1116–28.
[49] Lenes M, Koster L, Mihailetchi V, Blom P. Thickness dependence of the efficiency of polymer: fullerene bulk heterojunction solar cells. Appl Phys Lett 2006;88. [243502-243502].
[50] Hoppea H, Sariciftci NS. Organic solar cells: an overview. J Mater Res 2004;19:1925.
[51] Troshin P, Lyubovskaya R, Razumov V. Organic solar cells: structure, materials, critical characteristics, and outlook. Nanotechnol Russ 2008;3:242–71.
[52] Chandrasekaran J, Nithyaprakash D, Ajjan K, Maruthamuthu S, Manoharan D, Kumar S. Hybrid solar cell based on blending of organic and inorganic materials—an overview. Renew Sustain Energy Rev 2011;15:1228–38.
[53] Elumalai NK, Uddin A. Open circuit voltage of organic solar cells: an in-depth review. Energy Environ Sci 2016;9:391–410.
[54] Qi B, Wang J. Open-circuit voltage in organic solar cells. J Mater Chem 2012;22:24315–25.
[55] Ke J-C, Wang Y-H, Chen K-L, Huang C-J. Effect of open-circuit voltage in organic solar cells based on various electron donor materials by inserting molybdenum trioxide anode buffer layer. Sol Energy Mater Sol Cells 2015;133:248–54.
[56] Lo M, Ng T, Liu T, Roy V, Lai S, Fung M, et al. Limits of open circuit voltage in organic photovoltaic devices. Appl Phys Lett 2010;96:113303.
[57] Mihailetchi V, Blom P, Hummelen J, Rispens M. Cathode dependence of the open-circuit voltage of polymer: fullerene bulk heterojunction solar cells. J Appl Phys 2003;94:6849–54.
[58] Günes S, Neugebauer H, Sariciftci NS. Conjugated polymer-based organic solar cells. Chem Rev 2007;107:1324–38.
[59] Trukhanov VA, Bruevich VV, Paraschuk DY. Fill factor in organic solar cells can exceed the Shockley-Queisser limit. Sci Rep 2015;5.
[60] Qi B, Wang J. Fill factor in organic solar cells. Phys Chem Chem Phys 2013;15:8972–82.
[61] Gevorgyan SA, Madsen MV, Dam HF, Jørgensen M, Fell CJ, Anderson KF, et al. Interlaboratory outdoor stability studies of flexible roll-to-roll coated organic photovoltaic modules: stability over 10,000 h. Sol Energy Mater Sol Cells 2013;116:187–96.
[62] Rafique S, Abdullah SM, Sulaiman K, Iwamoto M. Layer by layer characterisation of the degradation process in PCDTBT: PC 71 BM based normal architecture polymer solar cells. Org Electron 2017;40:65–74.
[63] Norrman K, Madsen MV, Gevorgyan SA, Krebs FC. Degradation patterns in water and oxygen of an inverted polymer solar cell. J Am Chem Soc 2010;132:16883–92.
[64] Guerrero A, Boix PP, Marchesi LF, Ripolles-Sanchis T, Pereira EC, Garcia-Belmonte G. Oxygen doping-induced photogeneration loss in P3HT: PCBM solar cells. Sol Energy Mater Sol Cells 2012;100:185–91.
[65] Kim HJ, Lee HH, Kim JJ. Real time investigation of the interface between a P3HT: PCBM layer and an Al electrode during thermal annealing. Macromol Rapid Commun 2009;30:1269–73.

[66] Norrman K, Gevorgyan SA, Krebs FC. Water-induced degradation of polymer solar cells studied by H218O labeling. ACS Appl Mater Interfaces 2008;1:102–12.
[67] Glen T, Scarratt N, Yi H, Iraqi A, Wang T, Kingsley J, et al. Grain size dependence of degradation of aluminium/calcium cathodes in organic solar cells following exposure to humid air. Sol Energy Mater Sol Cells 2015;140:25–32.
[68] Ecker B, Nolasco JC, Pallarés J, Marsal LF, Posdorfer J, Parisi J, et al. Degradation effects related to the hole transport layer in organic solar cells. Adv Funct Mater 2011;21:2705–11.
[69] Jørgensen M, Norrman K, Krebs FC. Stability/degradation of polymer solar cells. Sol Energy Mater Sol Cells 2008;92:686–714.
[70] Morse GE, Tournebize A, Rivaton A, Chassé T, Taviot-Gueho C, Blouin N, et al. The effect of polymer solubilizing side-chains on solar cell stability. Phys Chem Chem Phys 2015;17:11884–97.
[71] Bao Q, Liu X, Braun S, Fahlman M. Oxygen-and water-based degradation in [6, 6]-phenyl-C61-butyric acid methyl ester (PCBM) films. Adv Energy Mater 2014;4.
[72] Guerrero A, Heidari H, Ripolles TS, Kovalenko A, Pfannmöller M, Bals S, et al. Shelf life degradation of bulk heterojunction solar cells: intrinsic evolution of charge transfer complex. Adv Energy Mater 2015;5.
[73] Madogni VI, Kounouhéwa B, Akpo A, Agbomahéna M, Hounkpatin SA, Awanou CN. Comparison of degradation mechanisms in organic photovoltaic devices upon exposure to a temperate and a subequatorial climate. Chem Phys Lett 2015;640:201–14.
[74] Kesters J, Verstappen P, Raymakers J, Vanormelingen W, Drijkoningen J, D'Haen J, et al. Enhanced organic solar cell stability by polymer (PCPDTBT) side chain functionalization. Chem Mater 2015;27:1332–41.
[75] Jeon SO, Lee JY. Improved lifetime in organic solar cells using a bilayer cathode of organic interlayer/Al. Sol Energy Mater Sol Cells 2012;101:160–5.
[76] Motaung DE, Malgas GF, Arendse CJ. Insights into the stability and thermal degradation of P3HT: C60 blended films for solar cell applications. J Mater Sci 2011;46:4942–52.
[77] Savagatrup S, Printz AD, O'Connor TF, Zaretski AV, Rodriquez D, Sawyer EJ, et al. Mechanical degradation and stability of organic solar cells: molecular and microstructural determinants. Energy Environ Sci 2015;8:55–80.
[78] Savagatrup S, Makaram AS, Burke DJ, Lipomi DJ. Mechanical properties of conjugated polymers and polymer-fullerene composites as a function of molecular structure. Adv Funct Mater 2014;24:1169–81.
[79] O'Connor B, Chan EP, Chan C, Conrad BR, Richter LJ, Kline RJ, et al. Correlations between mechanical and electrical properties of polythiophenes. ACS Nano 2010;4:7538–44.
[80] Zawacka NK, Andersen TR, Andreasen JW, Rossander LH, Dam HF, Jørgensen M, et al. The influence of additives on the morphology and stability of roll-to-roll processed polymer solar cells studied through ex situ and in situ X-ray scattering. J Mater Chem A 2014;2:18644–54.
[81] Tournebize A, Rivaton A, Peisert H, Chassé T. The crucial role of confined residual additives on the photostability of P3HT: PCBM active layers. J Phys Chem C 2015;119:9142–8.
[82] Wang X, Egelhaaf HJ, Mack HG, Azimi H, Brabec CJ, Meixner AJ, et al. Morphology related photodegradation of low-band-gap polymer blends. Adv Energy Mater 2014;4.
[83] Kim W, Kim JK, Kim E, Ahn TK, Wang DH, Park JH. Conflicted effects of a solvent additive on PTB7: PC71BM bulk heterojunction solar cells. J Phys Chem C 2015;119:5954–61.
[84] Elumalai NK, Saha A, Vijila C, Jose R, Jie Z, Ramakrishna S. Enhancing the stability of polymer solar cells by improving the conductivity of the nanostructured MoO3 hole-transport layer. Phys Chem Chem Phys 2013;15:6831–41.
[85] De Jong M, Van Ijzendoorn L, De Voigt M. Stability of the interface between indium-tin-oxide and poly (3, 4-ethylenedioxythiophene)/poly (styrenesulfonate) in polymer light-emitting diodes. Appl Phys Lett 2000;77:2255–7.
[86] Sharma A, Andersson G, Lewis DA. Role of humidity on indium and tin migration in organic photovoltaic devices. Phys Chem Chem Phys 2011;13:4381–7.
[87] Sharma A, Watkins SE, Lewis DA, Andersson G. Effect of indium and tin contamination on the efficiency and electronic properties of organic bulk heterojunction solar cells. Sol Energy Mater Sol Cells 2011;95:3251–5.
[88] Feron K, Nagle TJ, Rozanski LJ, Gong BB, Fell CJ. Spatially resolved photocurrent measurements of organic solar cells: tracking water ingress at edges and pinholes. Sol Energy Mater Sol Cells 2013;109:169–77.
[89] Voroshazi E, Verreet B, Buri A, Müller R, Di Nuzzo D, Heremans P. Influence of cathode oxidation via the hole extraction layer in polymer: fullerene solar cells. Org Electron 2011;12:736–44.
[90] Cheng P, Zhan X. Stability of organic solar cells: challenges and strategies. Chem Soc Rev 2016;45:2544–82.
[91] Mateker WR, Sachs-Quintana I, Burkhard GF, Cheacharoen R, McGehee MD. Minimal long-term intrinsic degradation observed in a polymer solar cell illuminated in an oxygen-free environment. Chem Mater 2015;27:404–7.
[92] Kong J, Song S, Yoo M, Lee GY, Kwon O, Park JK, et al. Long-term stable polymer solar cells with significantly reduced burn-in loss. Nat Commun 2014;5.
[93] Tipnis R, Bernkopf J, Jia S, Krieg J, Li S, Storch M, et al. Large-area organic photovoltaic module—fabrication and performance. Sol Energy Mater Sol Cells 2009;93:442–6.
[94] Roesch R, Eberhardt K-R, Engmann S, Gobsch G, Hoppe H. Polymer solar cells with enhanced lifetime by improved electrode stability and sealing. Sol Energy Mater Sol Cells 2013;117:59–66.
[95] Grossiord N, Kroon JM, Andriessen R, Blom PW. Degradation mechanisms in organic photovoltaic devices. Org Electron 2012;13:432–56.
[96] Parnell AJ, Cadby AJ, Dunbar AD, Roberts GL, Plumridge A, Dalgliesh RM, et al. Physical mechanisms responsible for the water-induced degradation of PC61BM P3HT photovoltaic thin films. J Polym Sci Part B: Polym Phys 2016;54:141–6.
[97] Seemann A, Sauermann T, Lungenschmied C, Armbruster O, Bauer S, Egelhaaf H-J, et al. Reversible and irreversible degradation of organic solar cell performance by oxygen. Sol Energy 2011;85:1238–49.
[98] Schafferhans J, Baumann A, Wagenpfahl A, Deibel C, Dyakonov V. Oxygen doping of P3HT: PCBM blends: influence on trap states, charge carrier mobility and solar cell performance. Org Electron 2010;11:1693–700.
[99] Kawano K, Pacios R, Poplavskyy D, Nelson J, Bradley DD, Durrant JR. Degradation of organic solar cells due to air exposure. Sol Energy Mater Sol Cells 2006;90:3520–30.
[100] Glatthaar M, Riede M, Keegan N, Sylvester-Hvid K, Zimmermann B, Niggemann M, et al. Efficiency limiting factors of organic bulk heterojunction solar cells identified by electrical impedance spectroscopy. Sol Energy Mater Sol Cells 2007;91:390–3.
[101] Yamanari T, Ogo H, Taima T, Sakai J, Tsukamoto J, Yoshida Y. Photo-degradation and its recovery by thermal annealing in polymer-based organic solar cells. In: Proceedings of the photovoltaic specialists conference (PVSC), 2010 35th IEEE, IEEE; 2010. p. 001628–31.
[102] Tamai Y, Ohkita H, Namatame M, Marumoto K, Shimomura S, Yamanari T, et al. Light-induced degradation mechanism in poly (3-hexylthiophene)/fullerene blend solar cells. Adv Energy Mater 2016;6.
[103] Norrman K, Larsen N, Krebs FC. Lifetimes of organic photovoltaics: combining chemical and physical characterisation techniques to study degradation mechanisms. Sol Energy Mater Sol Cells 2006;90:2793–814.
[104] Eloi CC, Robertson DJ, Rao AM, Zhou P, Wang K, Eklund PC. An investigation of photoassisted diffusion of oxygen in solid C 60 films using resonant alpha-scattering. J Mater Res 1993;8:3085–9.
[105] Córcoles L, Abad J, Padilla J, Urbina A. Wavelength influence on the photodegradation of P3HT: PCBM organic solar cells. Sol Energy Mater Sol Cells 2015;141:423–8.
[106] Madsen MV, Tromholt T, Norrman K, Krebs FC. Concentrated light for accelerated photo degradation of polymer materials. Adv Energy Mater 2013;3:424–7.
[107] Domínguez IF, Topham PD, Bussiere P-O, Bégué D, Rivaton A. Unravelling the photodegradation mechanisms of a low bandgap polymer by combining experimental and modelling approaches. J Phys Chem C 2015;119:2166–76.
[108] Tournebize A, Bussière PO, Wong-Wah-Chung P, Thérias S, Rivaton A, Gardette JL, et al. Impact of UV-visible light on the morphological and Photochemical behavior of a low-Bandgap poly (2, 7-carbazole) derivative for use in high--performance solar cells. Adv Energy Mater 2013;3:478–87.
[109] Deschler F, De Sio A, Von Hauff E, Kutka P, Sauermann T, Egelhaaf HJ, et al. The effect of ageing on exciton dynamics, charge separation, and recombination in P3HT/PCBM photovoltaic blends. Adv Funct Mater 2012;22:1461–9.
[110] Aygül U, Hintz H, Egelhaaf H-J, Distler A, Abb S, Peisert H, et al. Energy Level Alignment of a P3HT/Fullerene Blend during the Initial Steps of Degradation. J Phys Chem C 2013;117:4992–8.
[111] Rivaton A, Chambon S, Manceau M, Gardette J-L, Lemaître N, Guillerez S. Light-induced degradation of the active layer of polymer-based solar cells. Polym Degrad Stab 2010;95:278–84.
[112] Burlingame Q, Tong X, Hankett J, Slootsky M, Chen Z, Forrest SR. Photochemical origins of burn-in degradation in small molecular weight organic photovoltaic cells. Energy Environ Sci 2015;8:1005–10.
[113] Kumar A, Devine R, Mayberry C, Lei B, Li G, Yang Y. Origin of radiation-induced degradation in polymer solar cells. Adv Funct Mater 2010;20:2729–36.
[114] Kawano K, Adachi C. Evaluating carrier accumulation in degraded bulk heterojunction organic solar cells by a thermally stimulated current technique. Adv Funct Mater 2009;19:3934–40.
[115] Bruner C, Novoa F, Dupont S, Dauskardt R. Decohesion kinetics in polymer organic solar cells. ACS Appl Mater Interfaces 2014;6:21474–83.
[116] Awartani O, Lemanski BI, Ro HW, Richter LJ, DeLongchamp DM, O'Connor BT. Correlating stiffness, ductility, and morphology of polymer: fullerene films for solar cell applications. Adv Energy Mater 2013;3:399–406.
[117] Chung JY, Lee J-H, Beers KL, Stafford CM. Stiffness, strength, and ductility of nanoscale thin films and membranes: a combined wrinkling–cracking methodology. Nano Lett 2011;11:3361–5.
[118] Bruner C, Miller NC, McGehee MD, Dauskardt RH. Molecular intercalation and cohesion of organic bulk heterojunction photovoltaic devices. Adv Funct Mater 2013;23:2863–71.
[119] Dupont SR, Oliver M, Krebs FC, Dauskardt RH. Interlayer adhesion in roll-to-roll processed flexible inverted polymer solar cells. Sol Energy Mater Sol Cells 2012;97:171–5.
[120] Tanenbaum DM, Dam HF, Rösch R, Jørgensen M, Hoppe H, Krebs FC. Edge sealing for low cost stability enhancement of roll-to-roll processed flexible polymer solar cell modules. Sol Energy Mater Sol Cells 2012;97:157–63.
[121] Sapkota SB, Spies A, Zimmermann B, Dürr I, Würfel U. Promising long-term stability of encapsulated ITO-free bulk-heterojunction organic solar cells under different aging conditions. Sol Energy Mater Sol Cells 2014;130:144–50.
[122] Krebs FC. Encapsulation of polymer photovoltaic prototypes. Sol Energy Mater Sol Cells 2006;90:3633–43.
[123] Elkington D, Cooling N, Zhou X, Belcher W, Dastoor P. Single-step annealing and encapsulation for organic photovoltaics using an exothermically-setting encapsulant material. Sol Energy Mater Sol Cells 2014;124:75–8.
[124] Peters CH, Sachs-Quintana I, Kastrop JP, Beaupre S, Leclerc M, McGehee MD. High efficiency polymer solar cells with long operating lifetimes. Adv Energy Mater 2011;1:491–4.
[125] Romero-Gomez P, Betancur R, Martinez-Otero A, Elias X, Mariano M, Romero B, et al. Enhanced stability in semi-transparent PTB7/PC71BM photovoltaic cells. Sol

Energy Mater Sol Cells 2015;137:44–9.
[126] Kim T, Kang J, Yang S, Sung S, Kim Y, Park C. Facile preparation of reduced graphene oxide-based gas barrier films for organic photovoltaic devices. Energy Environ Sci 2014;7:3403–11.
[127] Aluicio-Sarduy E, Baidak A, Vougioukalakis GC, Keivanidis PE. Phosphorimetric characterization of solution-processed polymeric oxygen barriers for the encapsulation of organic electronics. J Phys Chem C 2014;118:2361–9.
[128] Zhao Z, Teki R, Koratkar N, Efstathiadis H, Haldar P. Metal oxide buffer layer for improving performance of polymer solar cells. Appl Surf Sci 2010;256:6053–6.
[129] Lattante S. Electron and hole transport layers: their use in inverted bulk heterojunction polymer solar cells. Electronics 2014;3:132–64.
[130] Yang H, Gong C, Guai GH, Li CM. Organic solar cells employing electrodeposited nickel oxide nanostructures as the anode buffer layer. Sol Energy Mater Sol Cells 2012;101:256–61.
[131] Meyer J, Zilberberg K, Riedl T, Kahn A. Electronic structure of Vanadium pentoxide: an efficient hole injector for organic electronic materials. J Appl Phys 2011;110:033710.
[132] Tan Za, Li L, Cui C, Ding Y, Xu Q, Li S, et al. Solution-processed tungsten oxide as an effective anode buffer layer for high-performance polymer solar cells. J Phys Chem C 2012;116:18626–32.
[133] Chen S, Manders JR, Tsang S-W, So F. Metal oxides for interface engineering in polymer solar cells. J Mater Chem 2012;22:24202–12.
[134] Kim J, Lee H, Lee SJ, da Silva WJ, bin Mohd Yusoff AR, Jang J. Graphene oxide grafted polyethylenimine electron transport materials for highly efficient organic devices. J Mater Chem A 2015;3:22035–42.
[135] Manders JR, Tsang SW, Hartel MJ, Lai TH, Chen S, Amb CM, et al. Solution-processed nickel oxide hole transport layers in high efficiency polymer photovoltaic cells. Adv Funct Mater 2013;23:2993–3001.
[136] Zilberberg K, Trost S, Schmidt H, Riedl T. Solution processed vanadium pentoxide as charge extraction layer for organic solar cells. Adv Energy Mater 2011;1:377–81.
[137] Girotto C, Voroshazi E, Cheyns D, Heremans P, Rand BP. Solution-processed MoO3 thin films as a hole-injection layer for organic solar cells. ACS Appl Mater Interfaces 2011;3:3244–7.
[138] Li S-S, Tu K-H, Lin C-C, Chen C-W, Chhowalla M. Solution-processable graphene oxide as an efficient hole transport layer in polymer solar cells. ACS Nano 2010;4:3169–74.
[139] Cheng C-E, Tsai C-W, Pei Z, Lin T-W, Chang C-S, Chien FS-S. UV-treated graphene oxide as anode interfacial layers for P3HT: PCBM solar cells. J Phys D: Appl Phys 2015;48:255103.
[140] Gao Y, Yip HL, Chen KS, O'Malley KM, Acton O, Sun Y, et al. Surface doping of conjugated polymers by graphene oxide and its application for organic electronic devices. Adv Mater 2011;23:1903–8.
[141] Lee D-Y, Na S-I, Kim S-S. Graphene oxide/PEDOT: PSS composite hole transport layer for efficient and stable planar heterojunction perovskite solar cells. Nanoscale 2016;8:1513–22.
[142] Rafique S, Abdullah SM, Mahmoud WE, Al-Ghamdi AA, Sulaiman K. Stability enhancement in organic solar cells by incorporating V 2 O 5 nanoparticles in the hole transport layer. RSC Adv 2016;6:50043–52.
[143] Wang M, Tang Q, An J, Xie F, Chen J, Zheng S, et al. ACS Performance and stability improvement of P3HT: PCBM-based solar cells by thermally evaporated chromium oxide (CrOx) interfacial layer. Appl Mater Interfaces 2010;2:2699–702.
[144] Li G, Chu C, Shrotriya V, Huang J, Yang Y. Efficient inverted polymer solar cells. Appl Phys Lett 2006;88. [253503-253503].
[145] Huang JH, Ibrahem MA, Chu CW. Wet-milled anatase titanium oxide nanoparticles as a buffer layer for air-stable bulk heterojunction solar cells. Progress Photovolt: Res Appl 2015;23:1017–24.
[146] Nikiforov MP, Strzalka J, Jiang Z, Darling SB. Lanthanides: new metallic cathode materials for organic photovoltaic cells. Phys Chem Chem Phys 2013;15:13052–60.
[147] Kim DY, Zinc oxide nanostructures for flexible and transparent electronics; 2014.
[148] Mbule P, Kim T, Kim B, Swart H, Ntwaeaborwa O. Effects of particle morphology of ZnO buffer layer on the performance of organic solar cell devices. Sol Energy Mater Sol Cells 2013;112:6–12.
[149] Wang DH, Kim JK, Seo JH, Park I, Hong BH, Park JH, et al. Transferable graphene oxide by stamping nanotechnology: electron-transport layer for efficient bulk-heterojunction solar cells. Angew Chem Int Ed 2013;52:2874–80.
[150] Jayawardena KI, Rhodes R, Gandhi KK, Prabhath MR, Dabera GDM, Beliatis MJ, et al. Solution processed reduced graphene oxide/metal oxide hybrid electron transport layers for highly efficient polymer solar cells. J Mater Chem A 2013;1:9922–7.
[151] Lu L, Zheng T, Wu Q, Schneider AM, Zhao D, Yu L. Recent advances in bulk heterojunction polymer solar cells. Chem Rev 2015;115:12666–731.
[152] Yu G, Gao J, Hummelen JC, Wudl F, Heeger AJ. Polymer photovoltiac cells: enhanced efficiencies via a network of internal donor-acceptor heterojunctions. Science 1995;270:1789.
[153] Ameri T, Khoram P, Min J, Brabec CJ. Organic ternary solar cells: a review. Adv Mater 2013;25:4245–66.
[154] Lu L, Kelly MA, You W, Yu L. Status and prospects for ternary organic photovoltaics. Nat Photonics 2015;9:491–500.
[155] An Q, Zhang F, Zhang J, Tang W, Deng Z, Hu B. Versatile ternary organic solar cells: a critical review. Energy Environ Sci 2016;9:281–322.
[156] He D, Du X, Zhang W, Xiao Z, Ding L. Improving the stability of P3HT/PC 61 BM solar cells by a thermal crosslinker. J Mater Chem A 2013;1:4589–94.
[157] Derue L, Dautel O, Tournebize A, Drees M, Pan H, Berthumeyrie S, et al. Thermal stabilisation of polymer–fullerene bulk heterojunction morphology for efficient photovoltaic solar cells. Adv Mater 2014;26:5831–8.
[158] Cheng YJ, Hsieh CH, Li PJ, Hsu CS. Morphological stabilization by in situ polymerization of fullerene derivatives leading to efficient, thermally stable organic photovoltaics. Adv Funct Mater 2011;21:1723–32.
[159] Chen CP, Huang CY, Chuang SC. Highly thermal stable and efficient organic photovoltaic cells with crosslinked networks appending open-cage fullerenes as additives. Adv Funct Mater 2015;25:207–13.
[160] Sivula K, Ball ZT, Watanabe N, Fréchet JM. Amphiphilic diblock copolymer compatibilizers and their effect on the morphology and performance of polythiophene: fullerene solar cells. Adv Mater 2006;18:206–10.
[161] Chen L, Tian S, Chen Y. Enhanced performance for organic bulk heterojunction solar cells by cooperative assembly of ter (ethylene oxide) pendants. Polym Chem 2014;5:4480–7.
[162] Ferenczi TA, Müller C, Bradley DD, Smith P, Nelson J, Stingelin N. Organic semiconductor: insulator polymer ternary blends for photovoltaics. Adv Mater 2011;23:4093–7.
[163] Jung JW, Jo JW, Jo WH. Enhanced performance and air stability of polymer solar cells by formation of a self-assembled buffer layer from fullerene-end-capped poly (ethylene glycol). Adv Mater 2011;23:1782–7.
[164] Kim J, Lee S, Nam S, Lee H, Kim H, Kim Y. A pronounced dispersion effect of crystalline silicon nanoparticles on the performance and stability of polymer: fullerene solar cells. ACS Appl Mater Interfaces 2012;4:5300–8.
[165] Peet J, Kim JY, Coates NE, Ma WL, Moses D, Heeger AJ, et al. Efficiency enhancement in low-bandgap polymer solar cells by processing with alkane dithiols. Nat Mater 2007;6:497–500.
[166] Dittmer JJ, Marseglia EA, Friend RH. Electron trapping in dye/polymer blend photovoltaic cells. Adv Mater 2000;12:1270–4.
[167] Nam S, Seo J, Woo S, Kim WH, Kim H, Bradley DD, et al. Inverted polymer fullerene solar cells exceeding 10% efficiency with poly (2-ethyl-2-oxazoline) nanodots on electron-collecting buffer layers. Nat Commun 2015;6.
[168] Dey S, Vivo P, Efimov A, Lemmetyinen H. Enhanced performance and stability of inverted organic solar cells by using novel zinc-benzothiazole complexes as anode buffer layers. J Mater Chem 2011;21:15587–92.
[169] Lee S-H, Seo J-W, Lee J-Y. Stable inverted small molecular organic solar cells using a p-doped optical spacer. Nanoscale 2015;7:157–65.
[170] Lan J-L, Cherng S-J, Yang Y-H, Zhang Q, Subramaniyan S, Ohuchi FS, et al. The effects of Ta2O5–ZnO films as cathodic buffer layers in inverted polymer solar cells. J Mater Chem A 2014;2:9361–70.
[171] Tavakkoli M, Ajeian R, Badrabadi MN, Ardestani SS, Feiz SMH, Nasab KE. Progress in stability of organic solar cells exposed to air. Sol Energy Mater Sol Cells 2011;95:1964–9.
[172] Yeom HR, Heo J, Kim G-H, Ko S-J, Song S, Jo Y, et al. Optimal top electrodes for inverted polymer solar cells. Phys Chem Chem Phys 2015;17:2152–9.
[173] De Sio A, Chakanga K, Sergeev O, Von Maydell K, Parisi J, Von Hauff E. ITO-free inverted polymer solar cells with ZnO: Al cathodes and stable top anodes. Sol Energy Mater Sol Cells 2012;98:52–6.